JOURNAL OF Materials CHEMISTRY

Ferromagnetism and magnetoresistance in monolayered manganites $Ca_{2-x}Ln_xMnO_4$

A. Maignan,[a] C. Martin,[a] G. Van Tendeloo,[b] M. Hervieu[a] and B. Raveau[a]

[a] *Laboratoire CRISMAT, UMR 6508 associée au CNRS, ISMRA et Université de Caen, 6 Boulevard du Maréchal Juin, 14050 Caen Cedex, France*
[b] *EMAT, University of Antwerp (RUCA), Groenenborgerlaan 171, B-2020 Antwerpen, Belgium*

Received 10th July 1998, Accepted 26th August 1998

Ferromagnetism (T_c) and negative magnetoresistive properties (maximum at 30 K) are observed in the monolayered manganites $Ca_{2-x}Ln_xMnO_4$ (Ln = Pr, Sm, Gd, Ho and $0 < x \leqslant 0.20$) despite their pure bidimensional character. A detailed structural study was carried out using X-ray diffraction, electron diffraction, and high resolution electron microscopy. This shows that they exhibit an orthorhombic cell, with $a \approx b \approx a_p\sqrt{2}$, $c \approx 12$ Å and *Aba*2 or *Abma* as possible space groups. In all these oxides, (001)-type twinning is observed, on a unit cell scale, creating in this way a local periodicity of 24 Å. In the $x = 0.08$ doped samples, it is observed that the microstructural state is strongly dependant on the synthesis process but it does not affect the magnetotransport properties.

Introduction

Numerous investigations performed recently on the manganites $Ln_{1-x}A_xMnO_3$ with the perovskite structure have shown their great ability to develop ferromagnetic metallic properties, allowing colossal magnetoresistance (CMR) to be generated. Such properties originate from double exchange (DE) interactions between Mn^{3+} and Mn^{4+} species.[1–5]

An important challenge is to modify the magnetoresistive properties of the manganites by introducing rock salt type layers between the octahedral layers, leading to layered manganites $(Ln,A)_{n+1}Mn_nO_{3n+1}$. In this respect, the study of the $n = 1$ member of this series, which exhibits the well known K_2NiF_4 structure is of great interest since it exhibits isolated $[MnO_2]_\infty$ layers. Consequently, its bidimensionality should reduce the 3d-bandwidth with respect to the 3D manganites, so that the hole mobility is decreased. From these considerations, a weakening of the DE interactions leading to the disappearance of CMR properties can be expected. The study of $La_{1-x}Sr_{1+x}MnO_4$ performed by Rao *et al.*[6,7] is of great interest. It shows that this compound is insulating and does not exhibit any ferromagnetic ordering but shows a spin glass transition around 20 K. Recently Moritomo *et al.*[8,9] confirmed the existence of a spin glass phase for this compound and showed the absence of magnetoresistance properties, in agreement with its bidimensional character.

Although the above results strongly support the absence of CMR effect in K_2NiF_4 type structure, owing to its bidimensionality, the possibility of inducing ferromagnetism in such oxides, by decreasing the thickness of the rock salt layer is worthwhile investigating. For this reason we have explored the manganites $Ca_{2-x}Ln_xMnO_4$, synthesised for the first time by Daoudi and Le Flem;[10] the small size of Ca^{2+} and Ln^{3+} cations (Ln = Pr, Nd, Sm, Gd) should indeed allow DE interactions to be enhanced. This investigation was also motivated by the fact that the electron doped tridimensional perovskites $Ca_{1-x}Ln_xMnO_3$ exhibit CMR properties.[11–13] In the present paper we show the existence of ferromagnetism and of negative magnetoresistive properties in the monolayered manganites $Ca_{2-x}Ln_xMnO_4$ in spite of their bidimensional character. A detailed structural study shows an orthorhombic symmetry and indicates that the existence of extended defects does not affect their magnetotransport properties.

Experimental

The manganites $Ca_{2-x}Ln_xMnO_4$ were investigated for Ln = Pr, Sm, Gd, Ho and for $0 \leqslant x \leqslant 0.20$, such that the electron concentration is not too high. The compounds were prepared from stoichiometric mixtures of CaO, Ln_2O_3 or Pr_6O_{11} and MnO_2 first heated at 1000 °C for 12 h, pressed into bars, sintered at 1200 °C, then at 1500 °C for 12 h and finally cooled down to room temperature at a rate of 1 °C min^{-1}. A second process was used for one of the compounds, $Ca_{1.92}Pr_{0.08}MnO_4$, in order to check the influence of the thermal treatment on the microstructural state and the magnetic properties. It partly differs from the above one only by the cooling rate: from 1500 to 800 °C at 5 °C min^{-1} and then quench to room temperature.

The purity and homogeneity of the sample were checked by X-ray diffraction (XRD) and electron diffraction (ED), coupled with energy dispersive spectroscopy (EDS). The XRD pattern was collected by means of a Philips diffractometer using Cu-Kα radiation, in the angular range $10 \leqslant 2\theta/^\circ \leqslant 110$, by steps of 0.02°.

The electron diffraction study was carried out with JEOL 200CX and 2010 electron microscopes, working at 200 kV. The high resolution electron microscopy study was carried out with a TOPCON electron microscope, having a point resolution of 1.8 Å. The samples were prepared by crushing the crystals in alcohol and the small flakes were deposited on a holey carbon film, deposited on a Cu grid. The three microscopes are equipped with EDS analysers.

Magnetization was measured with a vibrating sample magnetometer. The samples were first zero field cooled down to 5 K and then a magnetic field of 1.45 T was applied. The data were collected upon warming up to 300 K. AC susceptibility was registered with an AC-DC Quantum Design SQUID magnetometer. The resistance measurements were performed by a four-probe technique. Four contacts of indium were deposited on bars by using ultrasonic waves. The data were registered during cooling from 300 to 5 K in 0 and 7 T.

Results and discussion

Evidence for ferromagnetism and magnetoresistance effect

The evolution of the resistivity of the manganites $Ca_{2-x}Ln_xMnO_4$ *vs.* temperature in absence of magnetic field

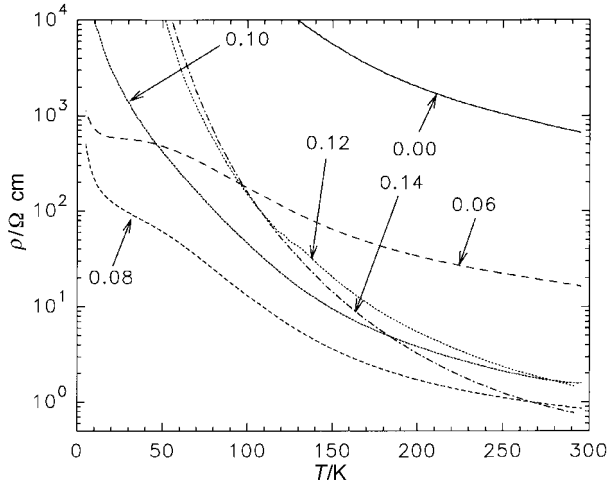

Fig. 1 T-dependent resistivity (ρ) of $Ca_{2-x}Pr_xMnO_4$ samples registered in earth magnetic field; x values are labelled on the graph.

is very similar whatever the nature of the lanthanide Ln = Pr, Sm, Gd or Ho. They all exhibit a semiconducting behaviour as illustrated for the praseodymium phases $Ca_{2-x}Pr_xMnO_4$ (Fig. 1). In the 200–250 K temperature domain, no inflection, which would correspond to a signature of charge ordering is observed on the $\rho(T)$ curves, in contrast to $La_{0.5}Sr_{1.5}MnO_4$.[14] The most important point is related to the shape of the $\rho(T)$ curves for low electron concentrations ($x = 0.05$ to 0.08), at low temperature. For these low x values a kind of plateau is observed between 50 and 20 K, followed by an upturn at the lower temperature, suggesting a re-entrant transition from an insulating to a semimetallic state.

The magnetization, registered under 1.45 T, *vs.* temperature [Fig. 2(a)] shows that the doping of Ca_2MnO_4 with electrons induces significant ferromagnetic interactions. Starting from the antiferromagnetic Ca_2MnO_4, the magnetic moment at 4.2 K increases as x increases, reaches 0.46 μ_B per mol of Mn for $x = 0.06$, remains practically constant in the range $0.06 \leqslant x \leqslant 0.10$, and finally decreases rapidly for $x > 0.10$, so that the ferromagnetic interactions for $x = 0.20$ have disappeared. Note, that the shape of the $M(T)$ curve for $x =$ 0.06–0.10, is different from that observed for a classical ferromagnetic transition, *i.e.* it is very smooth, in agreement with the fact that the magnetic moment at low temperature is far below the theoretical value (3.1 μ_B for $x = 0.10$) characteristic of a perfect ferromagnetic state. However, in a small ac-field of 10 Oe, the ferromagnetic transition is sharp and this $\chi'(T)$ curve allows one to determine the Curie temperature $T_C = 110$ K [Fig. 2(b)]. Moreover, the strong frequency dependence of the data below 105 K, together with the existence of a peak at 105 K seems to indicate that the sample must be considered as a cluster glass rather than a ferromagnet, as already reported for the $Ca_{1-x}Sm_xMnO_3$ perovskite for $x \leqslant 0.12$.[15]

The above results, existence of a ferromagnetic component and evidence for a re-entrant transition on the $\rho(T)$ curves, suggest the possibility of finding magnetoresistive properties for $0.06 \leqslant x \leqslant 0.12$. The $\rho(T)$ curves (Fig. 3) registered under 7 T support this viewpoint. The largest negative magnetoresistance is observed for $x = 0.06$ and 0.08 samples [Fig. 3(a), (b)] which exhibit practically identical $\rho(T)$ curves with a maximum resistivity ratio ($RR = \rho_0/\rho_{7T}$), $RR = 2.7$ at 40 K *i.e.* a magnetoresistance $MR = -64\%$, with $MR = (R_H - R_0)/R_0$. For $x =$ 0.12 [Fig. 3(c)] the negative magnetoresistance at 40 K is still similar, $MR = -50\%$ at 40 K. This maximum magnetoresistive effect for $0.06 \leqslant x \leqslant 0.12$ is in agreement with the ferromagnetism which is maximum for this composition range. Then, the magnetoresistance decreases rapidly as x increases, as shown

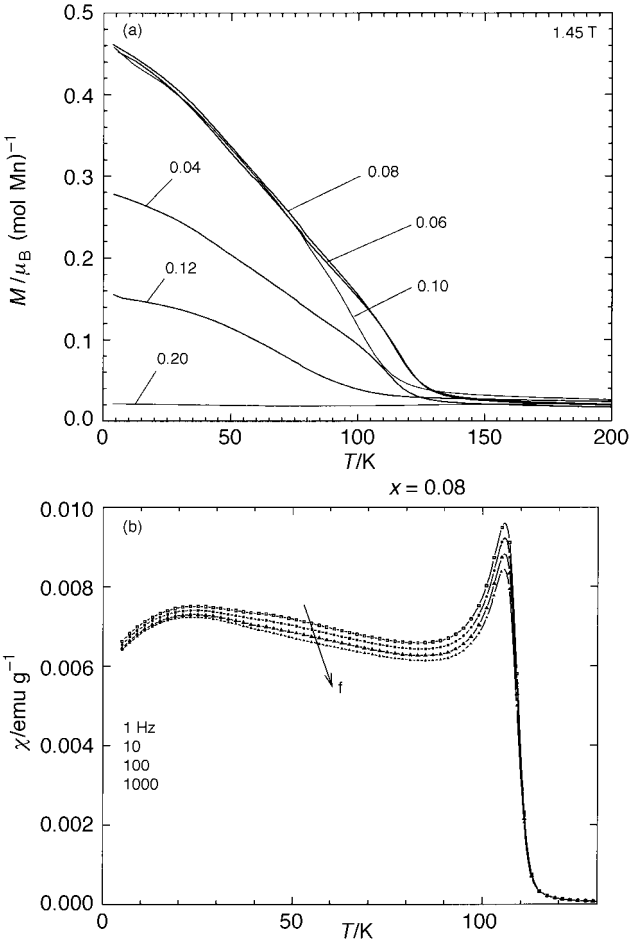

Fig. 2 (a) T-dependent magnetization (M) for the series $Ca_{2-x}Pr_xMnO_4$ (1.45 T); (b) ac-χ curves registered with $h_{ac} = 10$ Oe; frequencies are labelled on the graph.

for $x = 0.20$ [Fig. 3(d)]. The magnetoresistivity of these samples has also been confirmed from the $\rho(H)_T$ curves. An example is given for $Ca_{1.92}Pr_{0.08}MnO_4$ [inset of Fig. 3(b)]. These curves exhibit the reversibility of the magnetoresistance effect.

Very similar results are observed for all different lanthanides of the series Ln = Pr, Sm, Gd, Ho. For each, the highest ferromagnetic interactions are observed in the range $x =$ 0.08 − 0.10. They all exhibit a smooth $M(T)$ curve as illustrated in Fig. 4 for the oxides $Ca_{1.92}Ln_{0.08}MnO_4$. However, the most interesting result deals with the fact that the magnetic moment at 4.2 K increases linearly as the size of the lanthanide decreases, starting from 0.46 μ_B for Ln = Pr going through 0.56 μ_B and 0.64 μ_B for Ln = Sm and Gd, respectively, and reaching finally 0.70 μ_B for Ln = Ho. This size effect strongly supports our hypothesis that the thickness of the rock salt layer significantly influences the ferromagnetism in this one-layered structure. Doping with thorium (Th^{4+}) also indicates that the electron concentration plays a prominent role for the appearance of ferromagnetism. One indeed observes that the maximum magnetic moment of 0.44 μ_B, is obtained for the oxide $Ca_{1.96}Th_{0.04}MnO_4$ (Fig. 4), corresponding to the same electron concentration as the lanthanide based manganites $Ca_{1.92}Ln_{0.08}MnO_4$, assuming the tetravalence of thorium. For $Ca_{1.92}Th_{0.08}MnO_4$, the magnetic moment has already decreased down to 0.05 μ_B.

The increase of ferromagnetic interactions is not sufficient to increase significantly the magnetoresistance as the size of the lanthanide decreases. This is illustrated by comparing the $\rho(T)$ curves of the manganites $Ca_{1.92}Ln_{0.08}MnO_4$, registered under 0 and 7 T (with Ln = Sm and Ho in Fig. 5). One observes similar shapes of the $\rho(T)$ curves, characterised by a

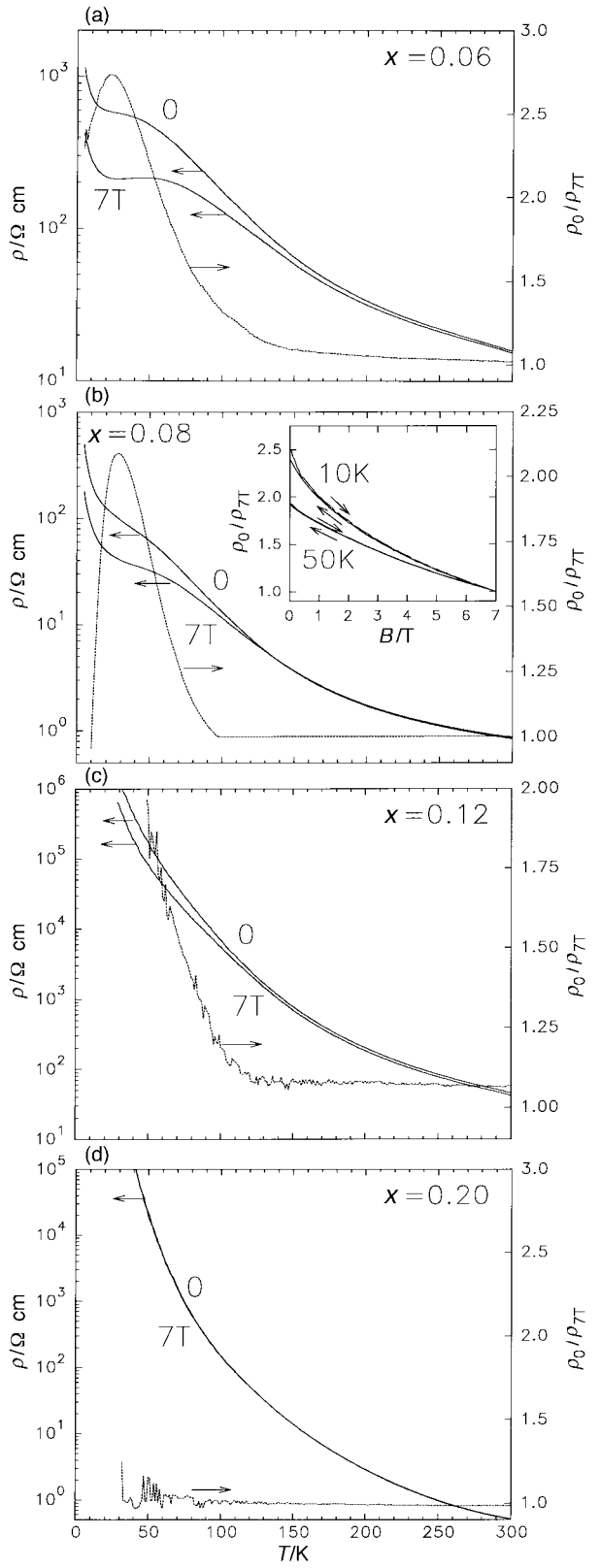

Fig. 3 $\rho(T)$ curves registered during cooling from 300 K down to 5 K in 0 and 7 T. The resistivity ratio $\rho(T)_{H=0}/\rho(T)_{H=7T}$ is also shown (right y-axis); (a) $Ca_{1.94}Pr_{0.06}MnO_4$, (b) $Ca_{1.92}Pr_{0.08}MnO_4$, (c) $Ca_{1.88}Pr_{0.12}MnO_4$ and (d) $Ca_{1.80}Pr_{0.20}MnO_4$. Inset of (b): isothermal magnetoresistance [$\rho(H)$ curves] registered for $T=10$ K, and $T=50$ K.

re-entrant transition around 40 K, and an upturn at 20 K. The resistivity ratio ρ_0/ρ_{7T} at 40 K is very similar, *i.e.* is *ca.* 3 for Sm [Fig. 5(a)] and Ho [Fig. 5(b)]. Note however that the maximum around 40 K is more clearly observed for Sm [Fig. 5(a)] than for Ho [Fig. 5(b)] or for Pr [Fig. 3(b)].

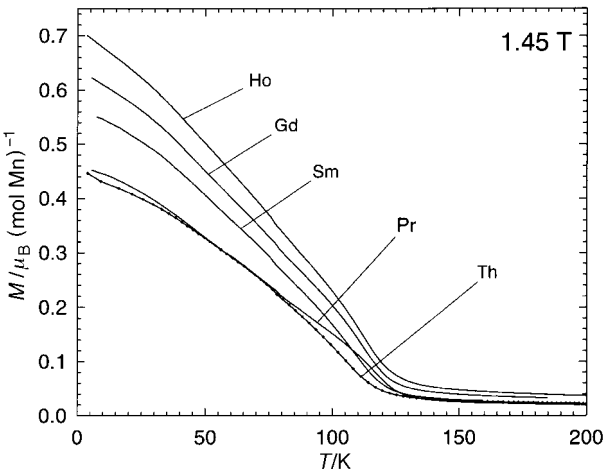

Fig. 4 $M(T)$ curves for the oxides $Ca_{1.92}Ln_{0.08}MnO_4$ with Ln = Pr, Sm, Gd and Ho and for $Ca_{1.96}Th_{0.04}MnO_4$ (Th curve).

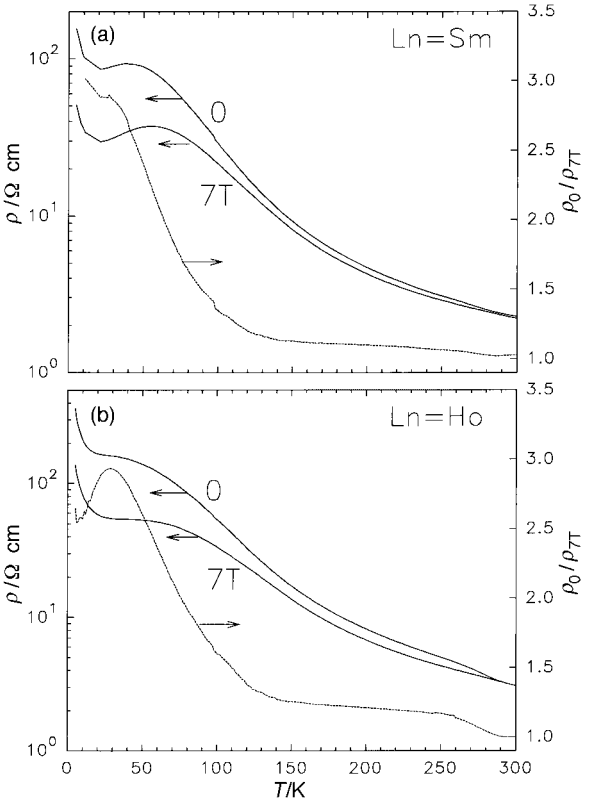

Fig. 5 $\rho(T)$ curves for two $Ca_{1.92}Ln_{0.08}MnO_4$ samples; (a) Ln = Sm and (b) Ln = Ho.

Structure and defects—relations with magnetoresistance properties

The main issue concerning the monolayered manganites $Ca_{2-x}Ln_xMnO_4$, is the origin of their magnetoresistance properties. Such properties may be intrinsic, or due to extended defects or inhomogeneities.[16] In order to answer this question a transmission electron microscopy (TEM) study is necessary.

For comparison, the pure Ca_2MnO_4 has been studied first. Remarkably enough, we could not confirm the tetragonal structure previously described.[17,18] We had to lower the symmetry to orthorhombic in order to index all diffraction patterns in a unit cell with lattice parameters $a\approx5.2$ Å, $b\approx5.2$ Å and $c\approx12.1$ Å. Diffraction evidence is presented in Fig. 6. Along the [001] zone [Fig. 6(a)], it is clear that the intensity of the reflections marked by two white triangles is not equal, violating the tetragonal symmetry; the very weak one belongs to a 90°

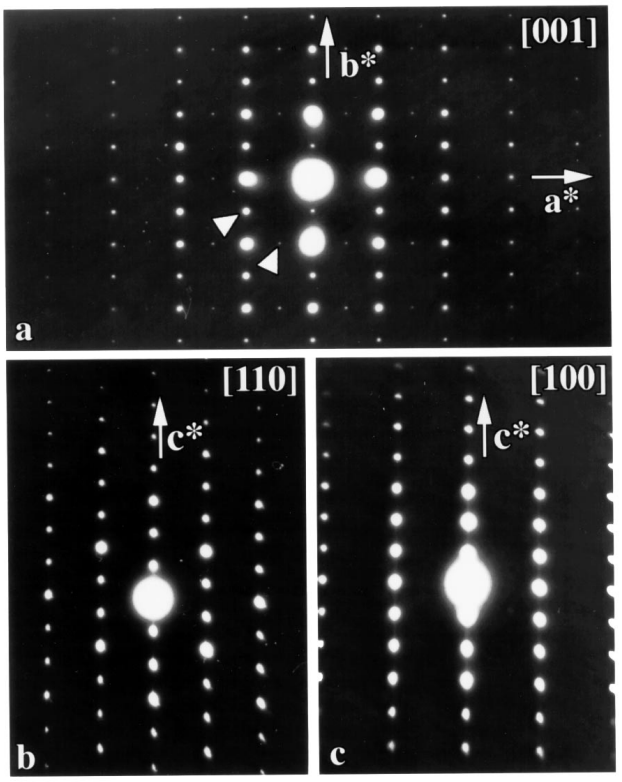

Fig. 6 Ca_2MnO_4: (a) [001], (b) [110] and (c) [100] ED patterns.

oriented domain. The weak reflections $h00$ and $0k0$ (h, $k=2n+1$) are present in this section due to double diffraction; this is clear from the [100] section in Fig. 6(c). The [110] zone is shown in Fig. 6(b). All these diffraction data show that the conditions limiting the reflection are $hkl: k+l=2n$, $0kl: k=2n$ and $h0l$ $h=2n$ and are compatible with space group *Aba*2 (no. 41) or *Abma* (no. 64).

Further convincing evidence for the orthorhombic symmetry comes from tilting about the c^* axis and dark field imaging along complex [$hk0$] zones [such as the zone in Fig. 7(a)] where additional weak reflections are clearly present in one row out of two. The pattern of Fig. 7(a) is again not compatible with a tetragonal symmetry. It can be interpreted on the basis of the superposition of the [$1\bar{2}0$] and [$2\bar{1}0$] zones, suggesting that twinning domains are systematically present in the crystallites. The 420 and 240 reflections are superposed due to the pseudo-tetragonal character of the cell ($a\approx b$); the weaker reflections [see the rows of dots indicated by arrows in Fig. 7(a)] are generated by the perovskite cell distortion ($a\approx b\approx a_p\sqrt{2}$). The A-type lattice implies the existence of the 120 and 122 reflections in the [$2\bar{1}0$] zone, the 121 being forbidden but the 211 is observed in the [$1\bar{2}0$] zone. In the bright (BF) and dark (DF) field images, given in Fig. 7(b) and (c), respectively, the basic (002) lattice fringes, separated by 6 Å are clearly resolved. Dark field imaging using several of these reflections produces images, with the 6 Å spaced fringes but where superimposed darker and lighter bands are visible. The width of these bands is hardly a few unit cells wide; they are the signature of the two orthorhombic variants, rotated 90° around the c-axis. Sometimes however, as in the area indicated A in Fig. 7(c), the twinning is locally periodic every 12 Å, creating in this way a local unit cell of 24 Å. The fact that this twinning, every 12 Å, is often on a unit cell scale, generating a doubling of the c parameter (24 Å) is to compare with the similar supercell '$a_p\sqrt{2}\times a_p\sqrt{2}\times 2c$' observed by Leonowicz *et al.*[17] on single crystals. Despite that the electron diffraction allows one to reject the hypothesis of the formation of such a double cell in our sample, the DF observations show a close relationship between the two structures. In fact, by applying the above periodic twinning mechanism to the orthorhombic *Aba*2 cell (present work) with $a\approx b\approx a_p\sqrt{2}$, $c\approx 12$ Å, we can create a P-type orthorhombic double cell with $a\approx b\approx a_p\sqrt{2}$, $2c\approx 24$ Å and space group *Pba*2. If we consider the atomic positions of the as-built structure, it appears that simply by constraining the y coordinate to the particular value $y=1/2-x$, we will generate a tetragonal cell with the space group $I4_1/acd$, which is identical with that previously proposed.[17,18] Structure calculations were therefore carried out in the *Aba*2 and $I4_1/acd$ space groups from the powder XRD data for

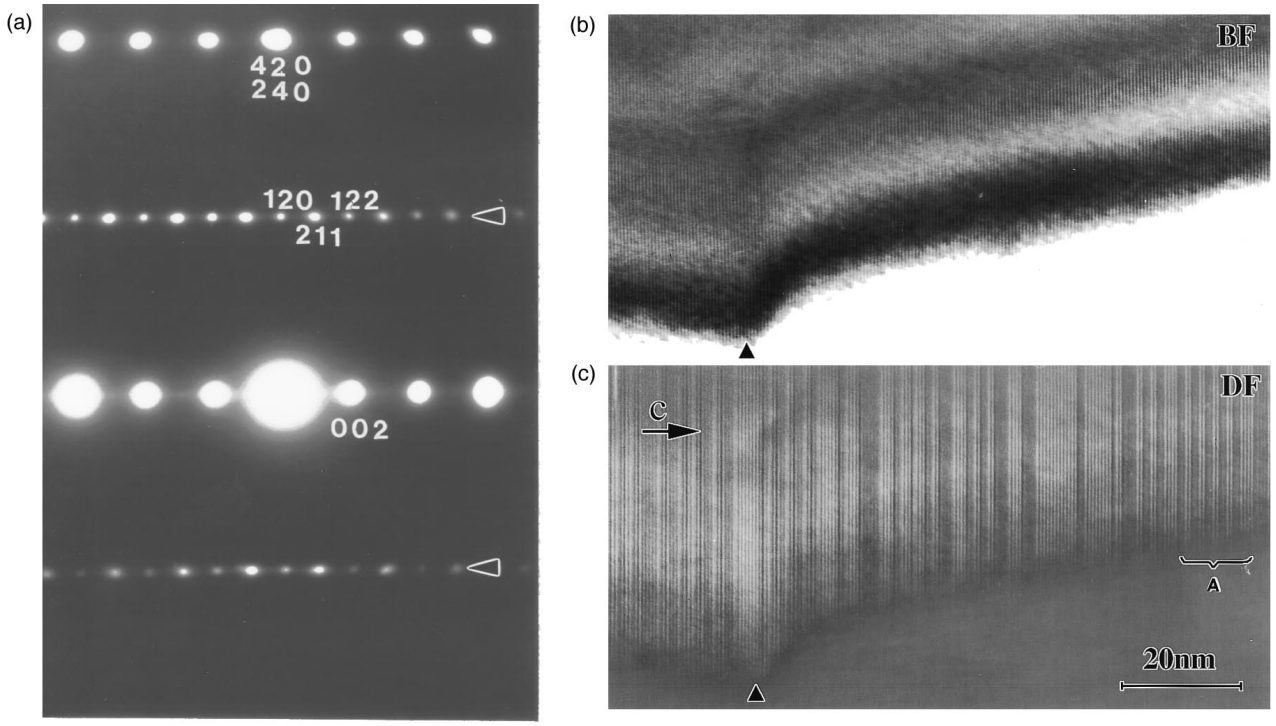

Fig. 7 Ca_2MnO_4: (a) enlarged ED pattern showing that the [$1\bar{2}0$] and [$2\bar{1}0$] zones are systematically superimposed, as the result of twinning phenomena; (b) bright and (c) dark field corresponding images.

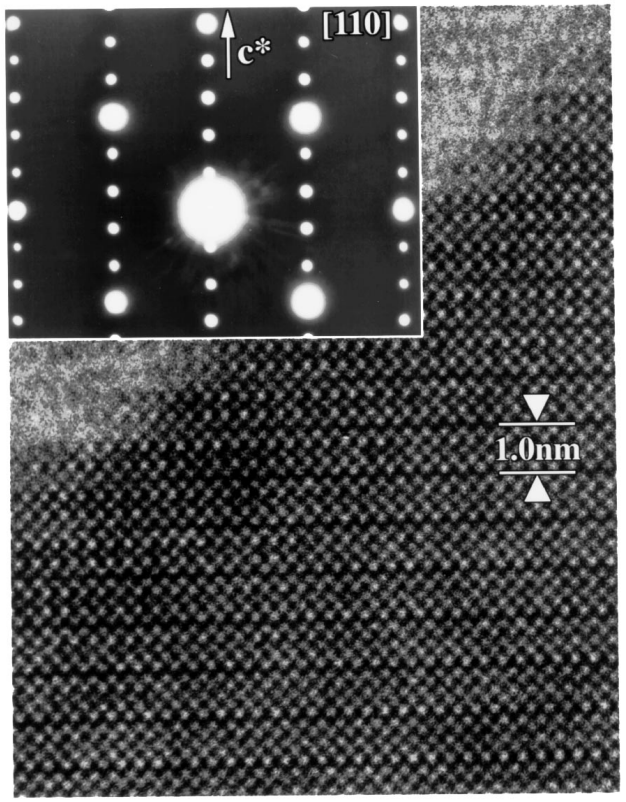

Fig. 8 $Ca_{1.92}Pr_{0.08}MnO_4$ sample: [110] ED pattern and HREM image, showing the characteristic contrast of the $n=1$ member of the $(Ca,Ln)_{n+1}Mn_nO_{3n+1}$ series. Most of the crystallites of the slowly cooled sample are defect free.

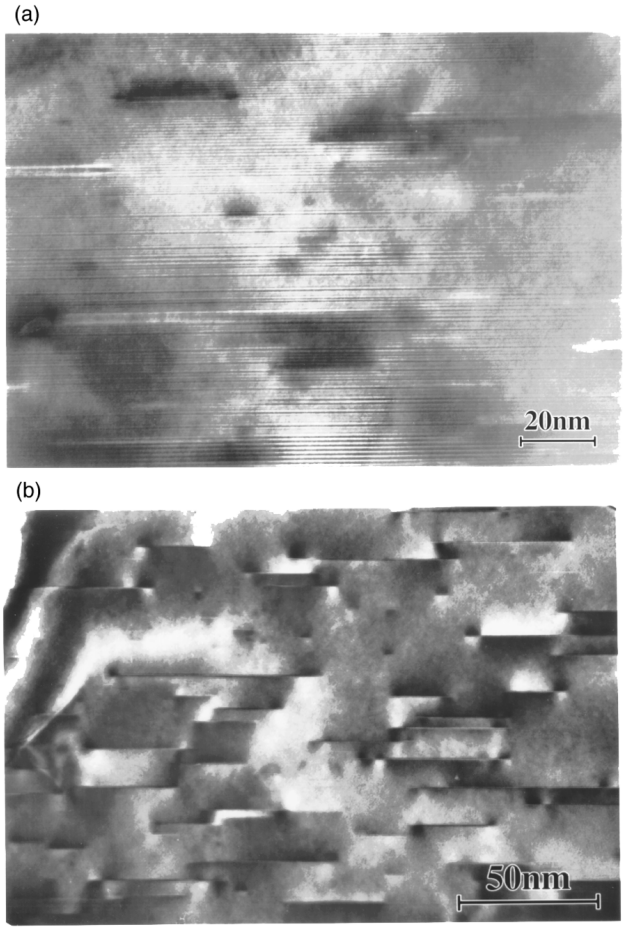

Fig. 9 Dark field images of the '800 °C-quenched' $Ca_{1.92}Pr_{0.08}MnO_4$ sample: (a) showing that the existence of twinning phenomena is not dependant on the thermal process (by selecting the weak extra reflections); (b) showing the existence of numerous defects and of the strain field associated with the pancake-like defects.

$Ca_{1.92}Sm_{0.08}MnO_4$ [$a=5.2206(11)$, $b=5.2195(11)$ and $c=12.0055(4)$Å for *Aba*2]. Both lead to reasonable R values, which attest to the validity of the model, but none allows an accurate refinement of the positions of the oxygen atoms located in the $[MnO_2]$ plane. Considering the complexity of the twinning system [Fig. 7(c)], it appears indeed impossible to get significant results from powder XRD data. Clearly, it seems that Leonowicz *et al.*,[17] obtained a different distortion of the Ca_2MnO_4 structure due to the fact that they worked at much lower temperature (900 °C instead of 1500 °C)and used a flux ($CaCl_2$).

Doping Ca_2MnO_4 with praseodymium or with gadolinium ($x=0.08$) and slowly decreasing the temperature (see Experimental section), produces the same remarkable microstructure. The overall bright field images show an even contrast with a very few extended defects, and the [110] HREM images exhibit the characteristic centring of the $n=1$ members of the $(Ln,A)_{n+1}Mn_nO_{3n+1}$ series, as the undoped Ca_2MnO_4 (Fig. 8). Only some occasional intergrowth defects corresponding to $n=3$ or $n=4$ members are detected. The dark field image, recorded according to the same conditions confirms the presence of numerous (001)-type twins, similar to the undoped material [Fig. 7(c)]. Apparently the orthorhombic symmetry is maintained. EDS analyses over relatively large areas (*ca.* 100 nm) confirm, in the limit of accuracy of the technique, that the cation ratio ($Ca/Ln\approx24$ and $Mn/Ca\approx0.52$) is in agreement with the nominal $Ca_{1.92}Ln_{0.08}MnO_4$ composition.

The absence of 3D perovskite and the very small number of intergrowth defects clearly show that the ferromagnetism and especially the magnetoresistance are intrinsic properties of the monolayered manganites $Ca_{2-x}Ln_xMnO_4$.

The possible influence of the presence of extended defects such as intergrowth members upon the properties of such samples has also been studied. For this study, we considered a second type of preparation. A $Ca_{1.92}Pr_{0.08}MnO_4$ sample was prepared following the same steps of the process as the other compounds, but was 'quenched' from 800 °C to room temperature. The EDS analyses showed that the actual composition is also very close to the nominal one. This '800 °C-quenched' $Ca_{1.92}Pr_{0.08}MnO_4$ sample exhibits exactly the same magnetotransport properties as the 'slowly cooled sample', whose microstructure is very regular, if one excepts the twinning phenomena. The dark field images show that the formation of (001)-type twins is not dependant on the cooling rate [Fig. 9(a)]. However their microstructure shows a different behaviour [Fig. 9(b)], involving the formation of 'pancake-like' defects along the [110] direction. The term 'pancake-like' refers to the dimensions of the defect, which is large along two directions (in the present case, a few nanometers) and small along the perpendicular direction. Along [110], it is clear that the internal structure of the defective area is perovskite like. The width of the defects is variable but never larger than two or three perovskite units [white triangle in Fig. 10(b)], corresponding to the local formation of $n=2$ and $n=3$ members of the $(Ln,A)_{n+1}Mn_nO_{3n+1}$ series. In a number of cases there is even no change in the periodicity of the basic Ca_2MnO_4 stacking, only a difference in intensity [see arrows in Fig. 10(a)]. The dark field images, taken with a smaller objective aperture [Fig. 9(b)] clearly indicate however that there is a strain field associated with most of the precipitates.

These results clearly show that the presence of pancake-like defects, correlated to the local formation of $n=2$ members of the series, and the associated strain fields do not affect the magnetotransport properties of these oxides.

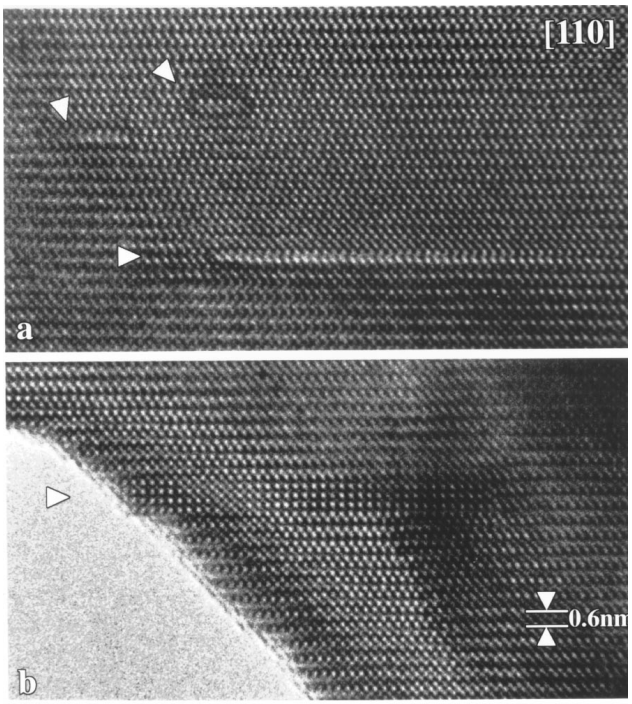

Fig. 10 Enlarged [110] HREM images of 'pancake-like' defects in $Ca_{1.92}Pr_{0.08}MnO_4$; (a) example of defects (see white triangles) which do not change the periodicity of the layer stacking, and only involve a local difference in intensity; (b) example of defect corresponding to the local formation of an $n=3$ member of the $(Ln,A)_{n+1}Mn_nO_{3n+1}$ series (white triangles).

The authors gratefully acknowledge the University of Caen, for supporting this work through a position of Associate Professor.

References

1 C. Zener, *Phys. Rev.*, 1951, **82**, 403.
2 P. W. Anderson and H. Hasegawa, *Phys. Rev.*, 1955, **100**, 675.
3 G. H. Jonker and J. H. Santen, *Physica*, 1950, **16**, 337.
4 P. G. de Gennes, *Phys. Rev.*, 1960, **118**, 141.
5 J. B. Goodenough, *Magnetism and the chemical bond*, John Wiley and Sons, New York–London, 1963.
6 C. N. R. Rao, P. Ganguly, K. K. Singh and R. A. M. Mohan Ram, *J. Solid State Chem.*, 1988, **72**, 14.
7 R. A. Mohan Ram, P. Ganguly and C. N. R. Rao, *J. Solid State Chem.*, 1987, **70**, 82.
8 Y. Moritomo, Y. Tomioka, A. Asamitsu and Y. Tokura, *Phys. Rev. B*, 1995, **51**, 3297.
9 Y. Moritomo, A. Asamitsu, H. Kuwahara and Y. Tokura, *Nature*, 1996, **340**, 141.
10 A. Daoudi and G. Le Flem, *J. Solid State Chem.*, 1972, **5**, 57.
11 I. O. Troyanchuk, N. V. Samsonesko, H. Szymczak and A. Nabialek, *J. Solid State Chem.*, 1997, **131**, 144.
12 C. Martin, A. Maignan, F. Damay and B. Raveau, *J. Solid State Chem.*, 1997, **134**, 198
13 A. Maignan, C. Martin, F. Damay and B. Raveau, *Chem. Mater.*, 1998, **10**, 950.
14 B. J. Sternlieb, J. P. Hill, U. C. Wildgruber, G. M. Luke, B. Nachumi, Y. Moritomo and Y. Tokura, *Phys. Rev. Lett.*, 1996, **76**, 2169.
15 A. Maignan, C. Martin, F. Damay, B. Raveau and J. Hejtmanek, *Phys. Rev. B*, 1998, **58**, 2758.
16 P. Laffez, G. Van Tendeloo, R. Seshadri, M. Hervieu, C. Martin, A. Maignan and B. Raveau, *J. Appl. Phys.*, 1996, **80**, 5850.
17 M. E. Leonowicz, K. R. Poeppelmeier and J. M. Longo, *J. Solid State Chem.*, 1985, **59**, 71.
18 J. Takahashi and N. Kamegashira, *Mater. Res. Bull.*, 1993, **28**, 565.

Paper 8/05393F